

Planar holographic optical processing devices

T. W. Mossberg*

LightSmyth Technology, Inc., Eugene, Oregon 97404

Received September 20, 2000

Time-domain optical processing implemented through linear spectral filtering offers unique potential for future high-bandwidth communications systems. One key to realization of this potential is the development of robust, cost-effective, fully integrated filtering devices. A new spectral filtering device concept, derived from the unique properties of index holograms stamped or otherwise written in thin planar waveguide slabs, is described. The holograms that are described provide for high-resolution spectral filtering while at the same time mapping general input spatial waveforms to desired output waveforms © 2001 Optical Society of America

OCIS codes: 200.4740, 230.7390.

Temporal-waveform processing devices¹⁻⁷ offer intriguing functionality that may be of use in developing optical communication areas such as code-division multiplexing^{8,9} and optical-layer decision making. In the following, a new type of integrated time-domain holographic optical processing device based on focusing planar waveguides is introduced. This device, which is referred to as a planar holographic optical processor (planar HOP), is uniquely compatible with low-cost, robust fabrication; packs multiple transfer functions within a single device; utilizes distinct input and output ports, thus eliminating the need for costly support devices such as optical circulators in processing applications; and operates on time scales that are useful in current optical communication systems.

A general optical processing (or filtering) device (OPD) as considered here is a device that applies a fixed or dynamically reprogrammable complex-valued spectral transfer function to an input signal. If $E_{in}(\nu)$ and $E_{out}(\nu)$ represent Fourier spectra of input and output signals, respectively, and $T(\nu)$ is a complex-valued spectral transfer function, the effect of the OPD can be represented as

$$E_{out}(\nu) = T(\nu)E_{in}(\nu). \quad (1)$$

The physical characteristics of a particular OPD determine the range and types of spectral transfer function that it can be configured to perform. The discussion here is restricted to OPD's that act to apply fully coherent transfer functions, i.e., devices that fully control the amplitudes and phases (except for an overall phase factor) applied to the input signal spectrum.

Previous OPD's have relied on free-space grating^{1,2} or coherent optical delay³⁻⁷ structures to achieve coherent optical filtering. These structures tend to be alignment sensitive and complex and (or) to provide limited spectral resolution. The planar HOP devices proposed here consist of one or more focusing holographic structures within or on a thin planar waveguide. Each holographic structure acts to accept light from a specific fiber-coupled input port, spectrally filter it, and direct it by imaging to a specific fiber-coupled output port. The planar HOP is completely integrated and robust and can be expected to support multiple overlaid holographic structures within a single device, each providing a separate spectral mapping from one or more input ports to one or more output ports. Although the

operative optical structures have a holographic character, fabrication can proceed by multiple means, including electron-beam master production with replication of copies. It is noted that spatial and spectral holographic structures have been shown to provide processing, filtering, and waveform storage functions but under quite different conditions.¹⁰⁻¹⁶ Similar function has been demonstrated in the quasi-one-dimensional environment of fibers.¹⁷⁻²¹

The essentials of a two-port planar HOP are shown schematically in Fig. 1(a). Light propagates in a thin slab (planar waveguide) of transparent substrate material lying in the $x-y$ plane. The planar waveguide confines waves to one or a few modes along the z direction. Optical signals are coupled into the planar grating device along its edge or via waveguide structures. Within the thin slab, a spatial index hologram acts to spectrally filter the input signal and spatially direct it to an output port. The constant index contours of the index hologram may have circular [see Fig. 1(a)], elliptical,²² or more-complex geometry. Control of the spacing and amplitude of

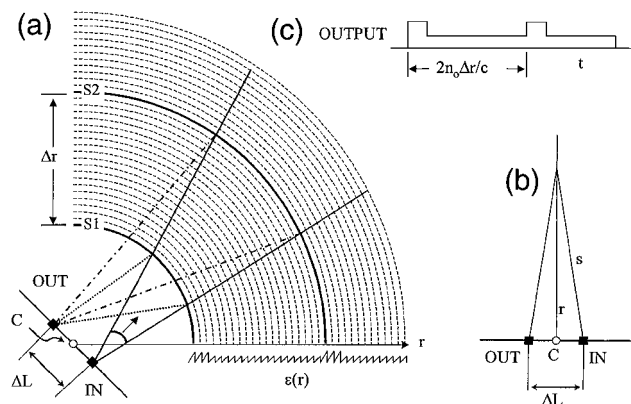


Fig. 1. (a) Schematic of planar HOP device. The arcs denote constant-index contours centered at C. Each arc, e.g., S1 and S2, images the input port to the output port. A representative spatial index variation $\epsilon(r)$ is shown. The actual spacing between successive contours is a multiple of $\lambda/2n_0$. (b) Optical path taken by a representative ray from input to output ports. The optical path length, s , is a function of r , the radial distance into the hologram. (c) Impulse response from the planar HOP, assuming the form of $\epsilon(r)$ shown in (a), except that the optical carrier is suppressed.

index variations provides required spectral filtering function. Index variations are created by modifications in the waveguide surface profile, in the surface profile of a thin overlaid layer, or in the actual bulk index of the waveguide. The use of surface modifications in the waveguide itself or in overlaid layers to create the index hologram is a possible path to very low-cost replication-based manufacture of planar HOP devices. Planar HOP devices complement the wide range of planar devices that are currently under development.^{23,24}

The arcs shown in Fig. 1(a) are contours of constant index. Point C is their common center and is assumed to lie midway along the segment, of length ΔL , connecting the input and output ports, which are represented by filled squares. The distance from the center of curvature, C, to an arbitrary point in the cylindrically symmetrical index hologram is denoted r . Viewing each constant-index arc as a reflective focusing mirror, we can see that the input and output ports are optically conjugate; i.e., each arc images the input port onto the output port. By making ΔL small, we can minimize small imaging aberrations. Then, Fermat's principle tells us that light backscattered from all points on a constant-index arc will have an identical input-output-port transit time. It follows that variation in index as a function of $2s(r)$, the optical distance between the input and output ports [see Fig. 1(b)], will translate directly into the optical impulse response of the device. Thus light not only is spatially mapped from the input to the output port but also spectrally filtered with a transfer function given by the Fourier transform of the impulse response, and hence the index variation with $s(r)$. Note that, for suitably small ΔL , $s(r) \approx r$.

To investigate the impulse response more quantitatively, we use the assumed cylindrical symmetry of the index, $n(r)$, to write

$$n(r) = n_0 + \varepsilon(r), \quad (2)$$

where n_0 is the average background index and it is assumed that $\varepsilon \ll n_0$. An impulsive signal of the form $E_0\delta(t)$, entering the input port and interacting with the index grating at position r along the line shown in Fig. 1(b), produces an output signal of amplitude $\alpha_c E_0 \varepsilon(r)$, which is delayed from the entrance time of the input signal by an r -dependent transit time given by $t(r) = 2n_0 s(r)/c$, where c is the vacuum light speed, α_c is a coupling constant, and $s(r)$ is the distance shown in Fig. 1(b). By use of the approximation

$$s(r) = r(1 + \Delta L^2/8r^2), \quad (3)$$

and with expressed r in terms of t , the output field produced by an impulsive input field is found to be

$$E_{\text{out}}(t) = \alpha_c E_0 \varepsilon \left[\frac{ct}{2n_0} - \eta(t) \right], \quad (4)$$

where $\eta(t) = \Delta L^2 n_0 / 4ct$. For suitably small ΔL , the output field mirrors in time the spatial variation of refractive index as a function of r . At the bottom of Fig. 1(a), a simple exemplary form of $\varepsilon(r)$ is shown. The spacing of index crests, actually a multiple of $\lambda/2n_0$, where λ is the operative vacuum wavelength,

is greatly exaggerated for visualization. The impulse response function produced by the exemplary $\varepsilon(r)$ is shown in Fig. 1(c), in which the two amplitude steps correspond to those in $\varepsilon(r)$. In Fig. 1(c), it is assumed that $\Delta L \ll r$ and the optical carrier is suppressed.

The transfer function of the planar HOP, $T(\nu)$, is the Fourier transform of Eq. (4):

$$T(\nu) = \frac{\alpha_c}{\sqrt{2\pi}} \int_{-\infty}^{\infty} \varepsilon \left[\frac{ct}{2n_0} - \eta(t) \right] \times \exp(2\pi i \nu t) dt. \quad (5)$$

In the limit that $\Delta L \ll 2(cr/\nu n_0)^{1/2}$, throughout the operative index hologram and frequency range the quantity $\eta(t)$ can be ignored. In this limit the temporal impulse response of the planar HOP is simply the Fourier transform of $\varepsilon(r)$. The index profile needed to produce a specific transfer function is obtained by inverse transformation of Eq. (5). Equations (4) and (5) are valid for moderate hologram reflectivity, since multiple scattering and depletion are ignored.

Note that the planar HOP of Fig. 1 has a maximal spectral resolution of $c/2n_0 D$, where D is the operative length of the holographic structure. Thus a 5-cm device in a silicon substrate offers a maximal spectral resolution of ~ 1 GHz. Realization of maximal spectral resolution for a given device size demands stringent control over the planar waveguide homogeneity and precision rendering of the holographic structure. Imperfections in either lead to lower device resolution, characterized by replacement of D with the distance over which $\lambda/2$ -scale optical path or positioning errors occur. Similar fabrication constraints apply even to simple diffraction gratings.

Parameterized as a function of transit delay, the index variation function may be represented as

$$\varepsilon(t) = A(t)f[t + p(t)], \quad (6)$$

where $A(t)$ is a real-valued, slowly varying amplitude function, $f(t) = f(t + \tau_g)$ is a real-valued periodic function whose minimal repeat period is τ_g and where $|p(t)| < \tau_g$ is a slowly varying function representing an r -dependent spatial phase shift in the hologram's quasi-periodic index variation. The index function versus r is obtained by the simple substitution $t = (2rn_0 + \Delta L^2 n_0 / 4r)/c$. Expanding $f(t)$ in a Fourier series,

$$\varepsilon(t) = A(t) \sum_{m=1}^{\infty} f_m \cos\{m\omega_g[t + p(t)] + \varphi_m\}, \quad (7)$$

where $\omega_g = 2\pi/\tau_g$, we can write a transfer function for each Fourier component of $\varepsilon(t)$ as

$$T_m(\nu) = \frac{\alpha_c f_m}{2\sqrt{2\pi}} \int_{-\infty}^{\infty} A(t) \times (\exp\{-im\omega_g[t + p(t)] - i\varphi_m\} + \text{c.c.}) \exp(2\pi i \nu t) dt. \quad (8)$$

Thus, provided that $f_m \neq 0$ for a particular value of m , the device exhibits an optical output with the indicated transfer function $T_m(\nu)$ at frequencies

$$\nu = \frac{m}{\tau_g} \cong \frac{mc}{2n_0\Lambda}, \quad (9)$$

where Λ is the minimal spatial interval over which the index is approximately spatially periodic. The output for $m = 1$ is first-order backdiffraction. Output frequencies for higher m correspond to higher backdiffraction orders and demonstrate that the physical grating spacing can be substantially greater than half the desired output wavelength in the substrate, provided that suitably high Fourier components are present in the index profile.

It should be noted that a planar HOP device possesses much more general spatial wave-front processing control capability that is apparent when simple cylindrically symmetrical index variations are used. The overall index structure is a two-dimensional hologram and has all the associated spatial transfer potential. One can engineer more-general index profiles to optimally map a general spatial input field to the desired output spatial mode, while at the same time applying a desired spectral transfer function. It is also important to note that planar HOP devices are immune, by virtue of their holographic character, to point defects introduced during use or fabrication. This property is supportive of robustness in use and high yield in fabrication.

The planar HOP concept supports multiple-port devices, with optical connections between the ports implemented with one or more focusing holographic structures. A single holographic structure can connect multiple-port pairs, provided that the elements of each port pair are located in optically conjugate positions of the structure. As shown in Fig. 1(a), various port pairs are simply placed symmetrically about point C, the holographic structure's center of symmetry. When different transfer functions are required for different connections, relevant ports are connected by separate holographic structures. Since index variations are assumed to be weak and the filtering process is linear, multiple holographic structures can be overlaid. As a special case of this capability, a single input port can be connected to a family of output ports by separate holographic structures, with each connection having a transfer function that tests (via, for example, cross correlation) the input signal for specific content. Such a configuration provides the basis for an optical packet decoder. In another special case, one input is connected to multiple outputs, with each connection being hologram specific to one or more specific wavelengths. Such a configuration represents an optical wavelength demultiplexer. In volume holographic studies, hundreds or even thousands of holograms have been written in the same spatial volume before cross-talk and insertion loss issues became limiting. Similar results may be anticipated in the case of planar HOP devices. Another advantage of the planar holographic approach is the ability, through use of semiconductor materials, to integrate optical and electronic processing onto a single substrate.^{23,24}

In conclusion, a powerful new planar design concept for time-domain OPD's has been presented. Devices

made with this design may be compatible with low-cost replication- (stamping-)based manufacture and provide multiple transfer functions in a single device, communications-scale frequency resolution in a small package, and highly reliable operation. New device concepts, together with ongoing progress in the methods of utilizing OPD's, may lead to substantial new capability in next-generation communication systems.

The author thanks W. R. Babbitt, T. Loftus, and M. G. Raymer for comments. His e-mail address is twmoss@mailaps.org.

*Also with the Department of Physics and Oregon Center for Optics, University of Oregon, Eugene, Oregon 97403.

References

1. W. R. Babbitt and T. W. Mossberg, *Opt. Commun.* **148**, 23 (1998).
2. A. M. Weiner, D. E. Leaird, D. H. Reitze, and E. G. Paek, *IEEE J. Quantum Electron.* **28**, 2251 (1992).
3. Y. L. Chang and M. E. Marhic, *J. Lightwave Technol.* **10**, 1952 (1992).
4. D. D. Sampson, R. A. Griffin, and D. A. Jackson, *J. Lightwave Technol.* **12**, 2001 (1994).
5. T. Kurokawa, H. Tsuda, K. Okamoto, K. Naganuma, H. Takenouchi, Y. Inoue, and M. Ishii, *Electron. Lett.* **33**, 1890 (1997).
6. W. D. Cornwell, N. Wada, K.-I. Kitayama, and I. Andonovic, *Electron. Lett.* **34**, 204 (1998).
7. J. Capmany and G. Mallea, *J. Lightwave Technol.* **17**, 570 (1999).
8. J. A. Salehi, A. M. Weiner, and J. P. Heritage, *J. Lightwave Technol.* **8**, 478 (1990).
9. M. E. Marhic, *J. Lightwave Technol.* **11**, 854 (1993).
10. Yu. T. Mazurenko, *Sov. Technol. Phys. Lett.* **10**, 228 (1984).
11. Yu. T. Mazurenko, *Appl. Phys. B* **50**, 101 (1990).
12. Yu. T. Mazurenko, *Opt. Eng.* **31**, 739 (1992).
13. T. W. Mossberg, *Opt. Lett.* **7**, 77 (1982).
14. Y. S. Bai, W. R. Babbitt, N. W. Carlson, and T. W. Mossberg, *Appl. Phys. Lett.* **45**, 714 (1984).
15. W. R. Babbitt and T. W. Mossberg, *Opt. Lett.* **20**, 910 (1995).
16. K. D. Merkel and W. R. Babbitt, *Opt. Lett.* **21**, 1102 (1996).
17. L. R. Chen, S. D. Benjamin, P. W. E. Smith, and J. E. Sipe, *IEEE J. Quantum Electron.* **34**, 2117 (1998).
18. L. R. Chen, P. W. E. Smith, and C. Martign de Sterke, *Appl. Opt.* **38**, 4500 (1999).
19. A. Grunnet-Jepsen, A. E. Johnson, E. S. Maniloff, T. W. Mossberg, J. J. Munroe, and J. N. Sweetser, *IEEE Photon. Technol. Lett.* **11**, 1283 (1999).
20. A. Grunnet-Jepsen, A. E. Johnson, E. S. Maniloff, T. W. Mossberg, M. J. Munroe, and J. N. Sweetser, *Electron. Lett.* **35**, 1096 (1999).
21. H. Fathallah, L. A. Rusch, and S. LaRochelle, *J. Lightwave Technol.* **17**, 397 (1999).
22. C. H. Henry, R. F. Kazarinov, Y. Shani, R. C. Kistler, V. Pol, and K. J. Orlowsky, *J. Lightwave Technol.* **8**, 748 (1990).
23. K. Kato and Y. Tohmori, *IEEE J. Sel. Top. Quantum Electron.* **6**, 4 (2000).
24. T. Miya, *IEEE J. Sel. Top. Quantum Electron.* **6**, 38 (2000).